Using multiple wavelengths for more precise detection of atmospheric wind phenomena

Albert Töws and Alfred Kurtz
Cologne University of Applied Sciences
Steinmüllerallee 1, 51643 Gummersbach, Germany
albert.toews@th-koeln.de

Abstract: An all-fiber multi-wavelength coherent Doppler lidar system in MOPA configuration with feedback controlled pulse shaping was developed and applied to wind measurements. The multi-wavelength system was designed to work with four wavelength-channels of the ITU-grid in the C-Band, which allow measurements along the same line-of-sight with different channel configurations. Those channels can be different in pulse shape, pulse length, and pulse repetition frequency (PRF). The resulting advantages and possibilities using multiple channels are: (1) All channels can be used simultaneously with the same pulse length and PRF to increase the effective PRF and therefore reduce the measurement time, enhance the detectability, or prevent ambiguity. (2) Atmospheric phenomena, such as wind shear, can be investigated with higher resolution using different pulse lengths.

Keywords: all-fiber coherent lidar, multi-wavelength, multi-channel, pulse-shape control

1. Introduction

In the past decade the 1.5 µm wavelength range has become broadly applied to pulsed coherent lidar systems due to the availability of components from the telecommunication industry. Since most of the telecommunication products are fiber based, cost effective all-fiber systems were developed. All-fiber lidar systems have successfully been commercialized, because of their compact size, mobility, low required maintenance, low cost components, and high reliability under vibrations and temperature variations [1, 2]. These systems work at lower pulse energy but at higher pulse repetition frequency (PRF) than systems based on free-space optics. However, a recently developed very large mode area (VLMA) fiber amplifier also achieves high pulse energies [3]. Thus, the peak and average power are pushed to the physical limits of such fiber amplifiers. Another possibility to enhance the performance of a lidar system is to increase the PRF. A higher PRF results in a reduced accumulation time or enhanced detectability. In single channel systems, the PRF defines the maximum range due to ambiguity of the return signal. Therefore, the effective PRF can only be increased using multiple parallel distinguishable channels. Two parallel channels can be created using two different polarization states [4]. In our lidar system, different wavelength-channels from the ITU-grid are simultaneously utilized. As already presented in [5], this system works with four independent channels.

2. Methodology

Figure 1 depicts the setup of the four-channel Doppler lidar system. Four laser diodes generate continuous-wave laser light in the master oscillator unit for each channel. The wavelengths are selected near 1.55 µm for low extinction in the atmosphere. All four channels are multiplexed and amplified by one erbium-doped fiber amplifier (EDFA). A part of that laser light is used as the local oscillator and the other part of the master oscillator laser light is guided to the pulse shaping unit. In the pulse shaping unit the laser light is demultiplexed, in order to separately shape the pulses of each channel with electro-optic modulators (EOM). Then, all pulses are frequency shifted and additionally shaped by an acousto-optic modulator (AOM). The shifted and shaped pulses are amplified with a three-stage EDFA. The output pulses to be

transmitted are monitored via a coupler and a feedback control system controls the EOMs, the AOM, and the pump power of the third EDFA stage. Therefore, arbitrary pulse shapes on every channel can be created and controlled.

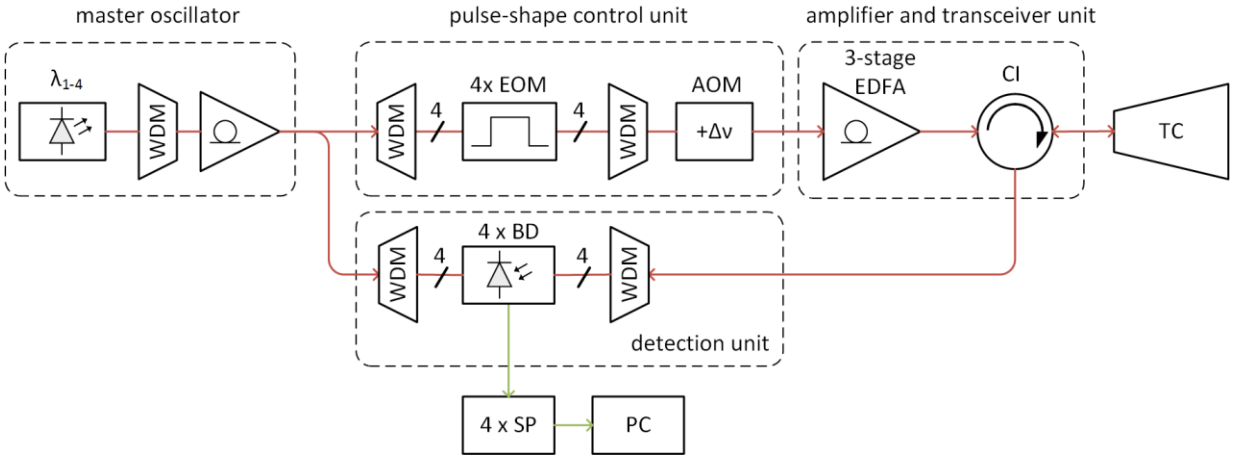

Figure 1. Overview of the multi-channel coherent Doppler lidar system.

Via a circulator (CI) the amplified and controlled pulses are directed to the telescope (TC). The backscattered light is guided to the detection unit, where the wavelengths of the local oscillator and the backscattered light are demultiplexed, thus, every channel can be mixed separately onto its balanced detector (BD). The amplified differential signal eliminates the DC and amplifies the AC component of the heterodyne signal. After analog signal processing (SP), the heterodyne signal is digitized and the raw data are sent to the personal computer (PC). An algorithm on the graphical processor extracts the information on wind velocity and signal strength in real time.

3. Multi-channel lidar system in high PRF mode

The signal-to-noise ratio (SNR) of atmospheric measurements with fiber-based lidar systems is typically below one. Hence, several pulses are transmitted successively and the measured data are averaged to enhance the detectability of the backscattered signal. The unambiguous range is $R_{max} = c/2f_{PRF}$, where f_{PRF} is the pulse repetition frequency (PRF) per channel. This is valid as long as the backscatter coefficient is constant along the line-of-sight. Under clear-air conditions the backscatter coefficient strongly decreases with height and the definition of the unambiguous range is correct. However, on cloudy days the return signal from clouds can be up to 25 dB higher [6]. If the chosen PRF is too high, those backscattered signals from clouds beyond the unambiguous range can significantly affect the measurement results.

An exemplary measurement in figure 2 shows the ambiguity due to a higher scatter intensity outside the unambiguous range. The abscissa represents the measurement time with a duration of 20 minutes, the ordinate the line-of-sight range, and the color bar in (a) the logarithmic signal amplitude and in (b) the measured radial velocity in the corresponding range gate. The depicted measurement starts with a PRF of 10 kHz and an elevation angle of 4°. With this configuration interfering signals from clouds were measured at a distance of about 3 km. The clouds were moving with ~8 m/s in the opposite direction to the wind close to the surface and are well visible in the velocity plot. After 6 minutes the elevation angle was changed to 30° for a duration of one minute. With this elevation angle the cloud ceiling was measured to be at an altitude of ~1600 m. From 8 to 16 minutes a PRF of 4 kHz and a 4° elevation angle were set to prevent ambiguity. The clouds appeared at a distance of about 18 km and no interfering signals were measured. By changing back to a PRF of 10 kHz, the backscattered signal from clouds beyond the unambiguous range appeared again at 2-3 km line-of-sight distance.

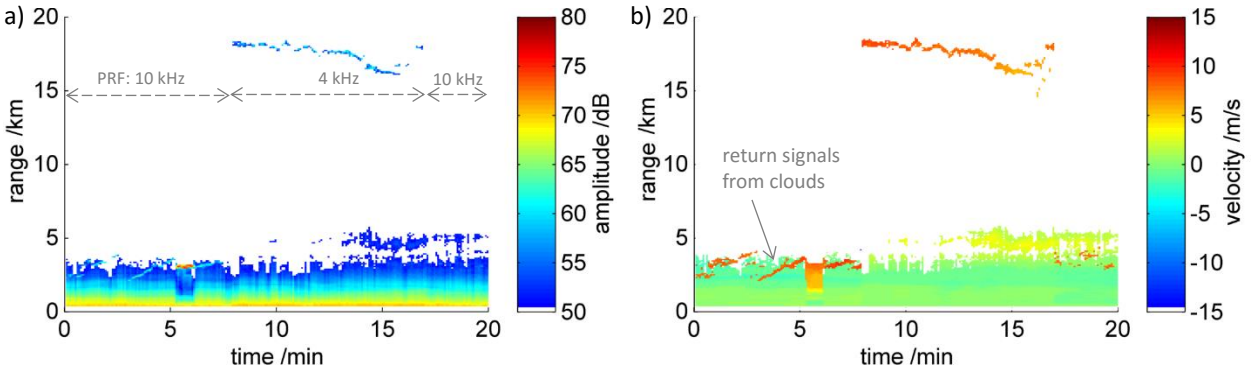

Figure 2. Measurement example of an ambiguity due to clouds.

To estimate the minimal required PRF, a constant backscatter coefficient of $1.3 \cdot 10^{-7}$ $m^{-1}sr^{-1}$ is assumed. This value increases to $2.2 \cdot 10^{-5}$ $m^{-1}sr^{-1}$ if clouds are the major scatterer [6]. The received SNR is predicted by the semianalytic lidar equation [7] with typical atmospheric values (one way transmittance: 0.96 km^{-1}, calm refractive turbulence parameter: $1 \cdot 10^{-16}$ $m^{-2/3}$) and shown in figure 3 as a function of range in black. The SNR of a cloud ceiling at 18 km distance is depicted in red. With an unambiguous range of 15 km the measured signal would appear at 3 km. Due to the higher SNR, the signal from outsight the unambiguous range significantly interferes with the clear-air signal in the vicinity of the lidar system. To suppress the probability of this disturbance, the PRF of single-channel coherent lidar systems has to be reduced to 4 kHz at least, which corresponds to an unambiguous range of 37.5 km. With this range the SNR of a cloud ceiling beyond the unambiguous range is >10 dB (blue) lower than the SNR of the clear-air scattering in the vicinity of the system and thus the interference would be negligible.

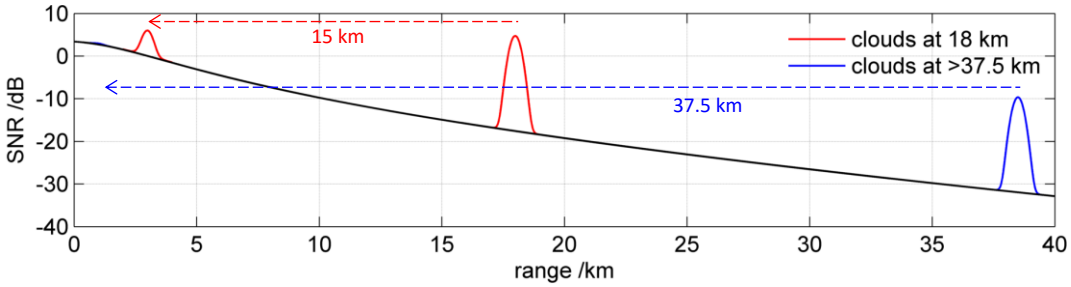

Figure 3. SNR as a function of range predicted by the lidar equation.

Due to the peak power limitation of fiber amplifiers, a lower PRF leads to lower detectability and thus to a longer required accumulation time. This downside of single-channel lidar systems is compensated by using multiple channels. With four independent channels the effective PRF is increased to 16 kHz with a corresponding unambiguous range of 37.5 km. Therefore, the multi-channel method reduces the probability of interference due to return signals from clouds outside the unambiguous range and enhances the performance of lidar systems commonly described by the basic figure-of-merit $FOM = E_P \cdot \sqrt{N \cdot f_{PRF}}$, where N is the number of channels and E_P the pulse energy per channel.

Principally, the number of channels is not limited with this multi-channel method and the PRF can be further increased. A possible limitation, using a single EDFA to amplify all channels simultaneously, is the required pump power. However, with multiple power amplifiers, for example one per channel, this limitation can be overcome.

4. Multi-channel observation with different pulse durations

This multi-channel lidar system enables atmospheric investigations with different pulse durations to be compared at the same time. For the following atmospheric measurement example, different pulse durations

on two channels of the multi-wavelength system were used. The chosen full-width half-maximum (FWHM) durations were 300 ns and 600 ns. The rise- and fall-time of the controlled pulses were 30 ns. Figure 4a shows the two amplified square shaped pulses. The measured pulse energies were 2.2 µJ (300 ns) and 4.3 µJ (600 ns). The exact rectangular FFT-window (FFT: fast Fourier transformation) size is identical to the pulse durations on each channel. The resulting range gate weighting function (RWF) is the convolution of the probing pulse and the FFT-window, and the effective longitudinal size of the sensing volume is defined at $\Delta z = \mathrm{RWF}(0)^{-1}$ [8]. The calculated RWFs for both measured probing pulses are depicted in 4b, which results in $\Delta z = 46.1$ m for the shorter pulse and $\Delta z = 91.1$ m for the longer pulse.

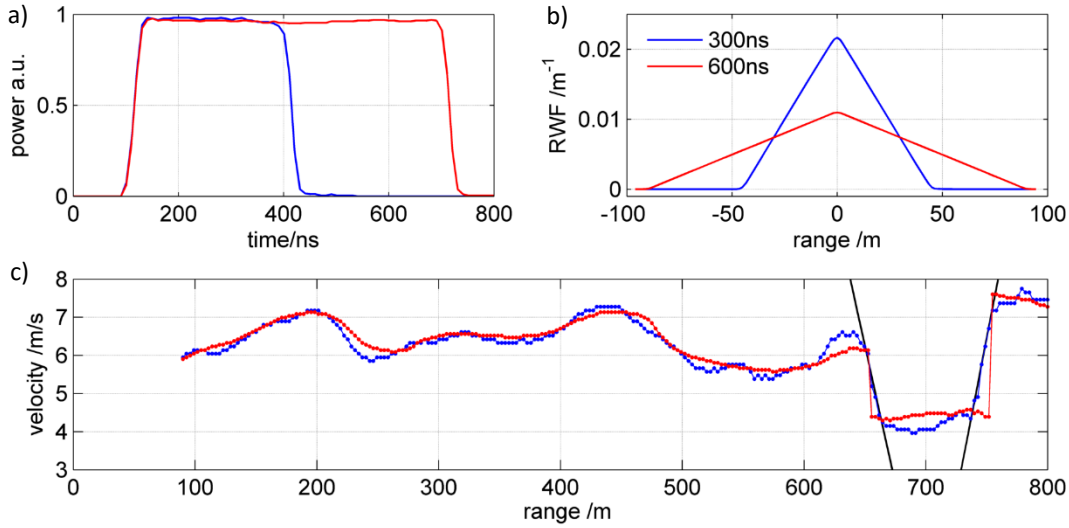

Figure 4. Atmospheric comparison measurement of different pulse durations.

The measured radial wind velocity over range is shown in figure 4c. The range gates were overlapped by 20 ns, which corresponds to a range resolution of 3 m for both channels. The shown line-of-sight velocity over range is the peak value of the averaged spectrum of 30,000 measurements. During that measurement the elevation angle was set to 5°.

As seen in 4a, the leading edges of both pulses are aligned. The measurement time for both pulses is equal to each pulse duration. Therefore, the first measurable range gate depicted in 4c corresponds to the center of both sensing volumes at 90 m. The channel with the longer pulse (red line) shows the wind structure more smoothed along the line-of-sight than the shorter pulse. A possible reason could be the influence of noise on the velocity precision. This was excluded by averaging the data for about 20 s to provide a velocity precision < 0.1 m/s over the whole range. The actual reason for the smoothing effect is the different size of the sensing volume of both channels. Due to the smaller sensing volume of the shorter pulse, the structure of the wind is determined in more detail. This can especially be seen around 650 m, where the blue channel estimates the velocity up to 0.5 m/s higher than the red channel.

In the vicinity of 700 m, strong changes of wind velocity are observed on both channels. Linear fitting to the velocity curve of the shorter pulse (black line) results in a wind shear dV/dz of -0.145 s^{-1} at 650 m and of 0.165 s^{-1} at a distance of 750 m. Despite the small depth of this shear, this change in velocity is referred to as low level wind shear in this paper, as it is defined by ICAO to 5 knots per 100 feet (0.085 s^{-1}) for moderate wind shear [9].

Using the multi-channel lidar with different pulse lengths, the longer pulses can be used to separate two existing wind velocities in one sensing volume, while with the shorter pulse the slope of those wind shears is determined more precisely. Figure 5 depicts these probing pulse properties in the frequency domain. 5a shows the wind shears measured with the longer pulse, where the velocities are well separated at 650 m and 750 m. In 5b, the spatial changes within the wind shears are measured more accurately. The center of the

wind shear is at the point where the longer pulse measures both wind components with the same weighting, assuming a constant particle density within the sensing volume. Using this method, the first wind shear location is at (656 ± 3) m and the second wind shear is at a range of (752 ± 3) m.

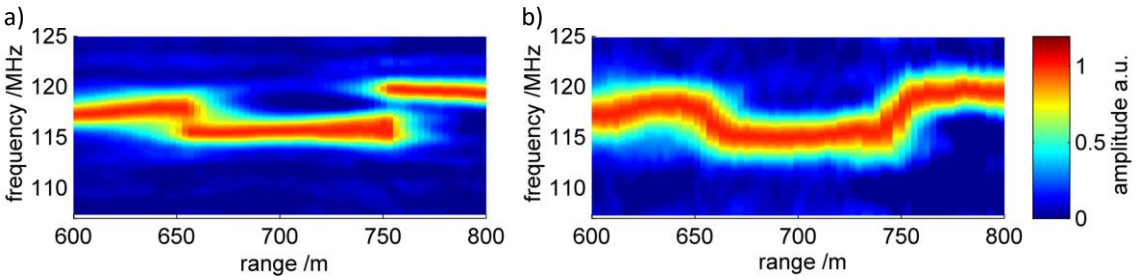

Figure 5. Measured wind shears in the frequency domain for different probing pulse lengths.

5. Conclusion

The developed multi-channel coherent Doppler lidar can be configured to work in high-PRF mode with enhanced unambiguous range and therefore performance is increased compared to conventional single-channel lidar systems. The channels of this multi-channel lidar can also be configured with different pulse lengths, allowing investigation of atmospheric phenomena with the corresponding Fourier-limited values.

6. References

[1] S. Kameyama, T. Ando, K. Asaka, Y. Hirano, and S. Wadaka, "Compact all-fiber pulsed coherent Doppler lidar system for wind sensing," Applied Optics, **46**, 1953-1962 (2007).

[2] N. S. Prasad, R. Sibell, S. Vetorino, R. Higgins, and A. Tracy, "An all-fiber, modular, compact wind lidar for wind sensing and wake vortex applications," in Laser Radar Technology and Applications XX; and Atmospheric Propagation XII, (Society of Photo-Optical Instrumentation Engineers, Baltimore, 2015), 94650C.

[3] D. Engin, B. Mathason, M. Stephen, A. Yu, H. Cao, J. Fouron, and M. Storm, "High energy, narrow linewidth 1572nm ErYb-fiber based MOPA for a multi-aperture CO_2 trace-gas laser space transmitter," in Fiber Lasers XIII: Technology, Systems, and Applications, Society of Photo-Optical Instrumentation Engineers, San Francisco, 2015), 97282S.

[4] C. F. Abari, X. Chu, R. M. Hardesty, and J. Mann, "A reconfigurable all-fiber polarization-diversity coherent Doppler lidar: principles and numerical simulations," Applied Optics, 54, 8999-9009 (2015).

[5] A. Töws and A. Kurtz, "A multi-wavelength LIDAR system based on an erbium-doped fiber MOPA-system," in Lidar Technologies, Techniques, and Measurements for Atmospheric Remote Sensing X, (Society of Photo-Optical Instrumentation Engineers, Amsterdam, 2014), 92460T.

[6] F. Boden, N. Lawson, H.W. Jentink, J. Kompenhans, *Advanced in-flight measurement techniques* (Springer, 2013), Chap. 12.

[7] S. Kameyama, T. Ando, K. Asaka, and Y. Hirano, "Semianalytic pulsed coherent laser radar equation for coaxial and apertured systems using nearest Gaussian approximation," Applied Optics, **49**, 5169-5174 (2010).

[8] V. Banakh and I. Smalikho, *Coherent Doppler wind lidars in a turbulent atmosphere* (Artech House, 2013).

[9] A. E. Richard, "Differentiating between types of wind shear in aviation forecasting," National Weather Digest, **24**(3), 39-51 (2000).